

Large-Scale Non-Gaussianities in the 21 cm Background Anisotropies From the Era of Reionization

Asantha Cooray

Theoretical Astrophysics, MS 130-33, California Institute of Technology, Pasadena, CA 91125.

Dept. of Physics and Astronomy, 4129 Frederick Reines Hall, University of California, Irvine, CA 92697.

E-mail: asante@caltech.edu

24 June 2018

ABSTRACT

The brightness temperature fluctuations in the 21 cm background related to neutral Hydrogen distribution provide a probe of physics related to the era of reionization when the intergalactic medium changed from a completely neutral to a partially ionized one. We formulate statistics of 21 cm brightness temperature anisotropies in terms of the angular power spectrum, the bispectrum, and the trispectrum. Using the trispectrum, we estimate the covariance related to the power spectrum measurements and show that correlations resulting from non-Gaussianities are below a percent, at most. While all-sky observations of the 21 cm background at arcminute-scale resolution can be used to measure the bispectrum with a cumulative signal-to-noise ratio of order a few ten, in the presence of foregrounds and instrumental noise related to first-generation interferometers, the measurement is unlikely to be feasible. For most purposes, non-Gaussianities in 21 cm fluctuations can be ignored and the distribution can be described by Gaussian statistics. Since 21 cm fluctuations are significantly contaminated by foregrounds, such as galactic synchrotron or low-frequency radio point sources, the lack of a significant non-Gaussianity in the signal suggests that any significant detection of a non-Gaussianity can be due to foregrounds. Similarly, in addition to frequency information that is now proposed to separate 21 cm fluctuations from foregrounds, if the non-Gaussian structure of foregrounds is a priori known, one can potentially use this additional information to further reduce the confusion.

Key words: cosmology: theory — diffuse radiation — large scale structure — intergalactic medium

1 INTRODUCTION

The 21 cm radio background related to spin-flip transition is a well-known probe of the neutral Hydrogen density content prior to and during the era of reionization (Scott & Rees 1990; Madau et al. 1997; Zaldarriaga, Furlanetto & Hernquist 2004; Morales & Hewitt 2004). This background has the advantage that by selecting the observed frequency of the redshifted line emission, one can directly view the neutral Hydrogen distribution of the Universe at a given redshift. With maps of the neutral Hydrogen content, as a function of the redshift, one can obtain statistics related to the reionization process, especially during the transition from a fully neutral medium to an ionized one (Barkana & Loeb 2001). Similarly, prior to the epoch of reionization when the Universe is fully neutral, 21 cm fluctuations pro-

vide a probe of the primordial density perturbations (Loeb & Zaldarriaga 2004; Bharadwaj & Ali 2004).

In addition to 21 cm data, information related to the era of reionization can be obtained with large angular scale cosmic microwave background (CMB) polarization observations. With CMB anisotropies, one is studying the presence of electrons through various Compton-scattering related processes where modifications are introduced to the temperature and polarization fluctuations. Unlike 21 cm observations, unfortunately, CMB data only allow a measurement of the integrated column density of electrons (Zaldarriaga 1997) with no detailed information on the exact reionization history of the universe (Hu & Holder 2003; Kaplinghat et al 2003). As has been studied recently, Lyman- α optical depth from Gunn-Peterson troughs (Gunn & Peterson 1965) towards $z \sim 6$ quasars in the Sloan Digital Sky Survey (Fan et al 2002) provides information related to

the end of reionization process when the Universe is almost fully ionized. While recent measurements from the WMAP mission (Bennett et al 2003) suggest an optical depth to electron scattering of 0.17 ± 0.04 (Kogut et al 2003), it can be explained with a variety of reionization models that also take into account the ionizing fraction estimates from $z \sim 6$ quasars (Cen 2003; Ciardi & Madau 2003; Chen et al 2003; Gnedin 2004; Wyithe & Loeb 2003; Haiman & Holder 2003).

With 21 cm observations, one can potentially reconstruct the exact reionization history and determine, especially, if the reionization process was either instantaneous or lengthy and complex as implied by current CMB and Sloan data. Moreover, since observable effects in CMB data depend only on the ionized content while 21 cm fluctuations come from inhomogeneities in the neutral distribution, the combination is expected to allow additional information related to the era of reionization (Cooray 2004; Cooray 2004). Detailed analytical and numerical studies related to the physics associated with the 21 cm background are now motivated by progress in the experimental side involving plans for a variety of low-frequency radio experiments such as PAST¹ (Pen 2004), Low Frequency Array (LOFAR)², and Square Kilometer Array (SKA)³.

While the scientific motivation to study 21 cm fluctuations during the era of reionization is strong, there are various challenges to overcome. These include the removal of foreground radio emission, such as due to synchrotron emission from the Milky Way (Shaver et al 1999), low frequency radio point sources (Di Matteo et al 2002) and free-free emission from free electrons in the intergalactic medium (Oh 1999; Cooray & Furlanetto 2004). Contrary to initial suggestions that 21 cm background studies may be impossible due to the large number of contaminating sources (Oh & Mack 2003), with brightness fluctuations much higher than expected for neutral Hydrogen at high redshifts, recent suggestions based on multifrequency analysis indicate that foreground contamination can be reduced given the smoothness of these confusions in frequency space (Shaver et al 1999; Di Matteo et al 2002; Zaldarriaga, Furlanetto & Hernquist 2004; Santos, Cooray & Knox 2004).

In current studies, the statistics related to 21 cm fluctuations have been mostly restricted to the angular power spectrum of anisotropies. This is primarily motivated by the expected Gaussian nature of these fluctuations. It is useful to consider if there are non-Gaussian signals in the 21 cm background anisotropies and, if any exists, whether these signals can be measured with planned low-frequency instruments. Here, we discuss the role of non-Gaussianities in the 21 cm background. For this purpose, we describe spatial fluctuations in the 21 cm background during the era of reionization as due to a combination of spatial fluctuations in the underlying neutral Hydrogen density, peculiar velocity of neutral gas, and the fraction of ionized gas relative to the total gas density. The non-Gaussian signals are generated by the non-

linear coupling of fluctuations in either the neutral density and peculiar velocity or neutral density and ionized-fraction fields.

We model the trispectrum, the Fourier analog of the four-point correlation function, of 21 cm anisotropies and explore how these non-Gaussianities affect the power spectrum measurement in terms of its full covariance. The trispectrum produces an additional source of noise beyond the standard cosmic variance under Gaussian statistics and correlates power spectrum measurements between different multipoles (Scoccimarro, Zaldarriaga & Hui 1999; Cooray & Hu 2001b). As we find, in the case of the 21 cm background, these correlations are at the level of at most a percent suggesting that non-Gaussianities are not likely to be a major source of complication when making a power spectrum measurement. We also estimate the bispectrum, the three-point correlation in Fourier space, of 21 cm anisotropies. While all-sky observations with no significant instrumental noise can be used to measure the bispectrum with signal-to-noise ratios of a few ten, for more practical observations with the first-generation of low-frequency radio interferometers, the signal-to-noise ratio is below a unity. In general, 21 cm background anisotropies can be described with Gaussian statistics and measurements can be focused primarily on the power spectrum. In our calculations, we mainly focus on the large physical, and thus large angular, scale fluctuations of the 21 cm background. Non-linear effects related to the neutral gas distribution and velocities can lead to additional non-Gaussian signals, but such effects are best captured in numerical simulations of the reionization process. These include the effects associated with finite size of reionized regions (c.f., Bharadwaj & Pandey 2004), and we leave these and other issues to be discussed in future works. For first-generation observations, such effects are unlikely to be important given restrictions on the angular resolution of observations. The lack of a significant non-Gaussianity at large angular scales, at least, has the advantage that if any significant non-Gaussianity is detected, it can be ascribed to foreground sources. Thus, in addition to smooth behavior in frequency space, the non-Gaussian structure of foregrounds, such as those related to Galactic synchrotron, can be used to further reduce the confusion.

The paper is organized as follows: in §2, we discuss the 21 cm signal anisotropy, the trispectrum in terms of the power spectrum covariance, and the bispectrum. While we only consider the non-Gaussian structure of the 21 cm background, the lack of a significant non-Gaussianity in the signal can be potentially used to separate nearby galactic foregrounds which are expected to be highly non-Gaussian. We discuss these and other possibilities in §3. Throughout the paper, we make use of the WMAP-favored Λ CDM cosmological model (Spergel et al 2003).

2 THE 21CM SIGNAL

The 21 cm surface brightness temperature observations are primarily observed as a change in the intensity of CMB due to line emission and absorption. The change in brightness

¹ <http://astrophysics.phys.cmu.edu/jbp>

² <http://www.lofar.org>

³ <http://www.skatelescope.org>

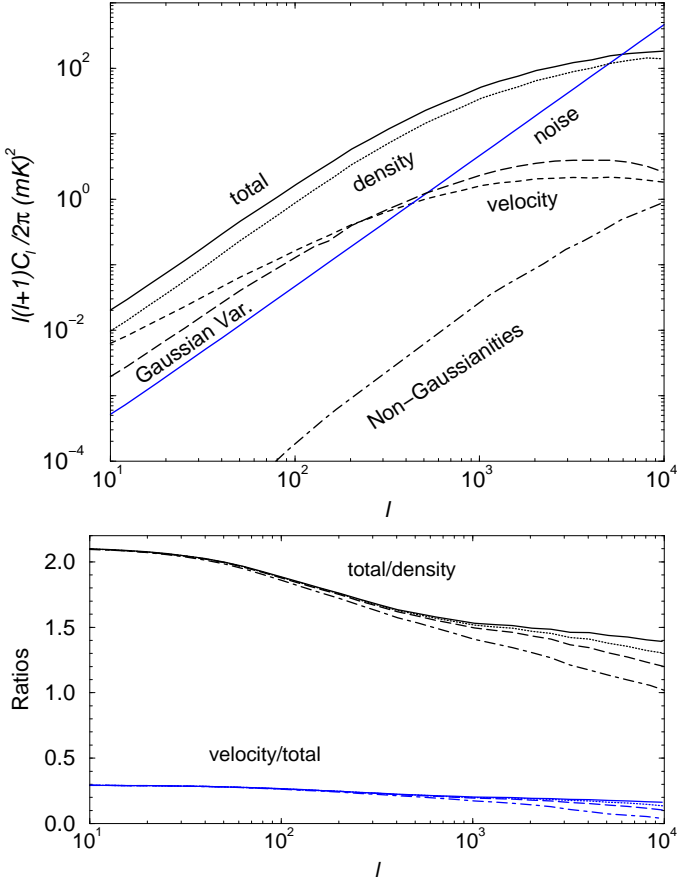


Figure 1. *Top:* The power spectrum for the 21cm signal at $z=10.0$ and assuming a bandwidth of $\delta\nu = 1\text{MHz}$. Units are in mK^2 . The calculation makes use of a reionization model from Santos, Cooray & Knox (2004), though similar results are obtained for slightly varying models from Santos et al. (2003). Here, we show the total contribution to the power spectrum (solid line), as well as the power spectrum related to neutral density (dotted line) and peculiar velocity (dashed line) fluctuations alone. We also show the Gaussian cosmic variance (long-dashed line) and an additional contribution to the power spectrum variance related to non-Gaussian trispectrum (dot-dashed line; see §2.1 for details). The solid line labeled 'noise' shows an estimated instrumental noise curve related to 21 cm observations with the SKA following Zaldarriaga, Furlanetto & Hernquist (2004). *Bottom:* The ratio of various contributions to the 21 cm anisotropy power spectrum. In the top curves, we show the ratio of total contribution to that related to density fluctuations alone, while the bottom set of curves are the ratio of peculiar velocity contribution to that of the total power spectrum. In each of these two sets, the four curves, from top to bottom, are for observational bandwidths of 0.1, 0.5, 1.0 and 2.5 MHz, respectively.

temperature, $T_{21}(\nu)$, compared to the CMB at an observed frequency ν is then

$$T_{21}(\nu) \approx \frac{T_S - T_{\text{CMB}}}{1+z} \tau \quad (1)$$

where T_S is the spin temperature of the IGM, z is the redshift corresponding to the frequency of observation ($1+z =$

ν_{21}/ν , with $\nu_{21} = 1420\text{ MHz}$) and $T_{\text{CMB}} = 2.73(1+z)K$ is the CMB temperature at redshift z .

In order to simplify the calculation related to 21 cm fluctuations, we assume that $T_s \gg T_{\text{CMB}}$, in a scenario where the gas density field in the intergalactic medium is heated as part of the reionization and structure formation processes. These include shocks associated with the formation of virialized dark matter halos where first stars are eventually found, and whose UV photons subsequently reionize the universe, and X-rays from first supernovae (Venkatesan, Giroux & Shull 2001; Chen & Miralda-Escudé 2004). At sufficiently high z , prior to significant reionization and heating, we expect $T_s < T_{\text{CMB}}$, and the HI density content is seen as an absorption in 21 cm with respect to the CMB (Madau et al. 1997). The statistics of 21 cm fluctuations related to such an early epoch can be used as a probe of primordial fluctuations (Loeb & Zaldarriaga 2004; Bharadwaj & Ali 2004).

The optical depth, τ , of this patch in the hyperfine transition (Field 1959) is given in the limit of $k_B T_s \gg h\nu_{21}$ by

$$\begin{aligned} \tau &= \frac{3c^3 \hbar A_{10} n_{\text{HI}}}{16k\nu_{21}^2 T_S H(z)} \quad (2) \\ &\approx 8.6 \times 10^{-3} \left(1 + \delta_g - \frac{1+z}{H(z)} \frac{\partial v}{\partial r} \right) x_H \left[\frac{T_{\text{CMB}}(z)}{T_S} \right] \\ &\quad \times \left(\frac{\Omega_b h^2}{0.02} \right) \left[\left(\frac{0.15}{\Omega_m h^2} \right) \left(\frac{1+z}{10} \right) \right]^{1/2} \left(\frac{h}{0.7} \right)^{-1}, \end{aligned}$$

where A_{10} is the spontaneous emission coefficient for the transition ($2.85 \times 10^{-15} \text{ s}^{-1}$), n_{HI} is the neutral Hydrogen density, and v is the peculiar velocity of the neutral gas distribution when r is the comoving radial distance and $H(z)$ is the expansion rate at a redshift of z . The neutral density be expressed as $n_{\text{HI}} = x_H \bar{n}_g (1 + \delta_g)$, when \bar{n}_g is the mean number density of cosmic baryons, with a spatially varying overdensity δ_g and x_H is the fraction of neutral Hydrogen ($x_H = 1 - x_e$ where x_e is the fraction of free electrons). We refer the reader to Zaldarriaga, Furlanetto & Hernquist (2004) and Santos, Cooray & Knox (2004) for further details. Note, however, that prior calculations related to the 21 cm anisotropies ignored both peculiar velocities and ionizing fraction fluctuations (e.g., Zaldarriaga, Furlanetto & Hernquist 2004), or peculiar velocities (Santos, Cooray & Knox 2004).

With $T_s \gg T_{\text{CMB}}$, the 21 cm signal will be observed in emission with respect to the background CMB. Writing the brightness temperature as:

$$T_{21}(z) = c \left(1 + \delta_g - \frac{1+z}{H(z)} \frac{\partial v}{\partial r} \right) (1 - \bar{x}_e - \bar{x}_e \delta_x), \quad (3)$$

where

$$c \approx 23 \left(\frac{\Omega_b h^2}{0.02} \right) \left[\left(\frac{0.15}{\Omega_m h^2} \right) \left(\frac{1+z}{10} \right) \right]^{1/2} \left(\frac{h}{0.7} \right)^{-1} \text{mK}, \quad (4)$$

and δ_x is the perturbation in the ionization fraction ($\delta_x \equiv \frac{x_e - \bar{x}_e}{\bar{x}_e}$). Here and above, the spatial dependent quantities are evaluated at the position $\mathbf{x} = r\hat{\mathbf{n}}$ and for simplicity in notation we have dropped this dependence.

The measured brightness temperature corresponds to a convolution of the intrinsic brightness with some response function $W_\nu(r)$ that characterizes the bandwidth of the experiment:

$$T(\hat{\mathbf{n}}, \nu_0) = \int dr W_{\nu_0}(r) T_{21}(\hat{\mathbf{n}}r, r), \quad (5)$$

where $\hat{\mathbf{n}}$ is the direction of observation and r corresponds to the observed frequency ν . We can now determine the angular power spectrum of $T(\hat{\mathbf{n}}, \nu_0)$ which is related to the 3-d power spectrum of $T_{21}(\hat{\mathbf{n}}, r)$, defined by

$$\langle \tilde{T}_{21}(\mathbf{k}, \nu_1) \tilde{T}_{21}(\mathbf{k}', \nu_2) \rangle = (2\pi)^3 \delta^D(\mathbf{k} + \mathbf{k}') P_{21}(k, \nu_1, \nu_2), \quad (6)$$

where $T_{21}(\hat{\mathbf{n}}, r) \equiv T_{21}(\mathbf{r}, \nu) = \int \frac{d^3\mathbf{k}}{(2\pi)^3} \tilde{T}_{21}(\mathbf{k}, \nu) e^{i\mathbf{k}\cdot\mathbf{r}}$.

Making use of the spherical harmonic moment of the 21 cm fluctuations, at a frequency ν_0 ,

$$a_{lm}(\nu_0) = \int d\hat{\mathbf{n}} Y_{lm}^*(\hat{\mathbf{n}}) T(\hat{\mathbf{n}}, \nu_0), \quad (7)$$

we define the angular power spectrum as (Kaiser 1992)

$$\langle a_{lm}(\nu_1) a_{lm}^*(\nu_2) \rangle = C_l(\nu_1, \nu_2). \quad (8)$$

To calculate this power spectrum, first, we write Fourier space fluctuations in the brightness temperature as

$$\begin{aligned} T_{21}(\mathbf{k}, z) = & c [\delta_g(\mathbf{k})(1 - \bar{x}_e) + \mu^2 \delta_v(\mathbf{k})(1 - \bar{x}_e) - \bar{x}_e \delta_x(\mathbf{k}) \\ & - \bar{x}_e \int \frac{d^3\mathbf{k}'}{(2\pi)^3} \delta_x(\mathbf{k}') \delta_g(\mathbf{k} - \mathbf{k}') \\ & - \bar{x}_e \mu'^2 \int \frac{d^3\mathbf{k}'}{(2\pi)^3} \delta_x(\mathbf{k}') \delta_v(\mathbf{k} - \mathbf{k}')] \end{aligned} \quad (9)$$

where δ_v is the velocity divergence, $\mu = \hat{\mathbf{n}} \cdot \hat{\mathbf{k}}$, and $\mu' = \hat{\mathbf{n}} \cdot (\hat{\mathbf{k}} - \hat{\mathbf{k}}')$. Here, we concentrate primarily on the large scale velocity fluctuations and at these scales, we can use linear theory to write $\delta_v(\mathbf{k}) = f(\Omega_m) \delta^{\text{lin}}(\mathbf{k})$ where $f(\Omega_m) \equiv \partial \ln G / \partial \ln a \approx \Omega_m^{0.6} + 1/70 [1 - 1/2\Omega_m(1 + \Omega_m)]$, where G is the growth factor related to evolution of density perturbations with the approximation valid in a flat cosmology with a cosmological constant.

To calculate the power spectrum of 21 cm fluctuations, we ignore terms which are second order and higher and involving the convolution between density and ionization-fraction and velocity and ionization-fraction fluctuations. We make use of the Rayleigh expansion for the plane wave given by

$$e^{i\mathbf{k}\cdot\mathbf{r}} = 4\pi \sum_{lm} i^l j_l(kr) Y_l^m(\hat{\mathbf{n}}) Y_l^{m*}(\hat{\mathbf{k}}), \quad (10)$$

and separately consider fluctuations in the velocity and density fields separately. To simplify the calculation associated with the velocity fluctuations, we also use

$$\hat{\mathbf{n}} \cdot \hat{\mathbf{k}} = \sum_m \frac{4\pi}{3} Y_1^m(\hat{\mathbf{n}}) Y_1^{m*}(\hat{\mathbf{k}}). \quad (11)$$

After straightforward, but tedious, algebra, we can write the power spectrum as

$$C_l(\nu_1, \nu_2) = \frac{2}{\pi} \int k^2 dk$$

$$\begin{aligned} & \times \left\{ P_{aa}(k, \nu_1, \nu_2) I_l^{\nu_1}(k) I_l^{\nu_2}(k) + P_{bb}(k, \nu_1, \nu_2) J_l^{\nu_1}(k) J_l^{\nu_2}(k) \right. \\ & \left. + P_{ab}(k, \nu_1, \nu_2) [I_l^{\nu_1}(k) J_l^{\nu_2}(k) + J_l^{\nu_1}(k) I_l^{\nu_2}(k)] \right\} \end{aligned} \quad (12)$$

where

$$\begin{aligned} I_l^\nu(k) &= \int dr W_\nu(r) j_l(kr) \\ J_l^\nu(k) &= \int dr W_\nu(r) j_l''(kr), \end{aligned} \quad (13)$$

with the spherical Bessel function given by $j_l(kr)$. In deriving Eq. 12, we have ignored terms which are second order in δ . In Eq. 13, the double derivative of the spherical Bessel function is with respect to its argument.

The corresponding three-dimensional power spectra are

$$\begin{aligned} P_{aa}(k, z) &= c^2 [(1 - \bar{x}_e)^2 P_{gg}(k, z) + \bar{x}_e^2 P_{\delta_x \delta_x}(k, z) \\ &\quad - 2P_{g\delta_x}(k, z) \bar{x}_e (1 - \bar{x}_e)], \\ P_{bb}(k, z) &= c^2 [(1 - \bar{x}_e)^2 P_{\delta_v \delta_v}(k, z)], \\ P_{ab}(k, z) &= c^2 [(1 - \bar{x}_e)^2 P_{g\delta_v}(k, z) - P_{\delta_v \delta_x}(k, z) \bar{x}_e (1 - \bar{x}_e)]. \end{aligned} \quad (14)$$

The neutral Hydrogen density power spectrum is represented by $P_{gg}(k, z)$, $P_{\delta_x \delta_x}(k, z)$ is the power spectrum related to perturbations in the ionized fraction, $P_{g\delta_x}(k, z)$ is the cross-correlation power between these two, and $P_{\delta_v \delta_v}(k, z)$ is the velocity divergence spectrum. Using linear theory evolution of gravitational perturbations, the latter can be written as $P_{\delta_v \delta_v}(k, z) \approx f^2(\Omega_m) P^{\text{lin}}(k, z)$ in terms of the linear density spectrum. The cross spectra between velocity and neutral density and ionized fraction are given as $P_{g\delta_v}$ and $P_{\delta_v \delta_x}(k, z)$, respectively.

We assume the neutral Hydrogen density field is an unbiased tracer of the dark matter density field and write $P_{gg}(k, z) = P_{\delta\delta}(k, z)$ and, when illustrating our results, use the linear theory spectrum to describe dark matter around the era of reionization. More complicated models that capture the non-linear behavior of the gas density field can be obtained through approaches such as the halo models of large scale structure (Cooray & Sheth 2002), but extended to higher redshifts. Note that the correlations in the ionized fraction depend on the reionization history and we make use of the patchy reionization model in Santos et al (2003) to write

$$P_{\delta_x \delta_x}(k, z) = b^2(z) P_{\delta\delta}(k, z) e^{-k^2 R^2} \quad (15)$$

where $b(z)$ is a mean bias that captures the halo bias (Mo et al. 1997) weighted by the different halo properties, and R the mean radius of the HII patches. The time-dependence of R is modeled as $R = \left(\frac{1}{1 - \bar{x}_e}\right)^{1/3} R_p$ where R_p is the (co-moving) size of the fundamental patch taken to be ~ 100 Kpc.

In addition to the power spectra of the gas density, velocity divergence, and ionization fraction, when presenting numerical results, we assume cross-correlation spectra between each of these three fields can be described with perfect correlations such that for example, $P_{xy} = \sqrt{P_{xx} P_{yy}}$ where x and y are any of the two fields of interest.

In Fig. 1, we show the power spectrum of 21 cm fluctuations at a redshift of 10 with a bandwidth for observations

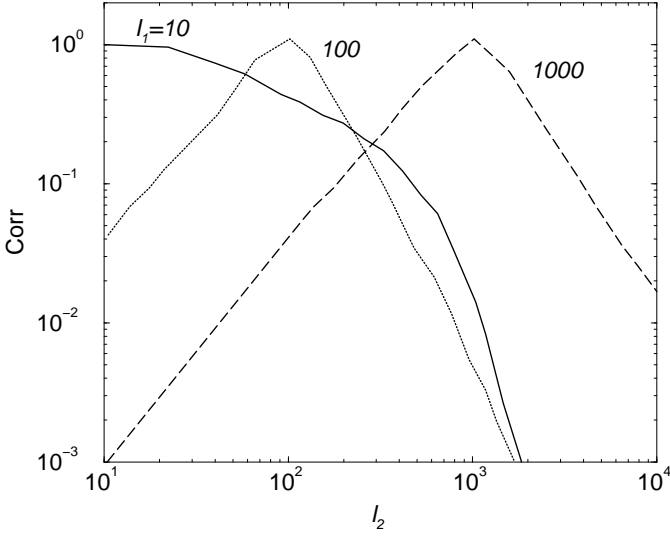


Figure 2. The correlation coefficients related to the non-Gaussian covariance of 21 cm power spectrum measurements at $z = 10$ with a bandwidth for observations of 1 MHz. Here, we show $\text{Cov}_{l_1 l_2}^{\text{NG}} / \sqrt{\text{Cov}_{l_1 l_1}^{\text{NG}} \text{Cov}_{l_2 l_2}^{\text{NG}}}$ as a function of l_2 when $l_1 = 10, 100,$ and 1000 . Note that these are correlations only in the non-Gaussian part of the contribution to the covariance. The total correlations, when considering the measurement of the 21 cm angular power spectrum, include the part due to Gaussian variance. Since Gaussian variance is roughly two orders of magnitude or more higher than that of non-Gaussianities, as shown in Fig. 1, these correlations are at most a percent and can be ignored for all practical purposes.

of 1 MHz. Here, we make use of a reionization model from Santos, Cooray & Knox (2004), but similar results, with amplitudes varying as shown in Fig. 2 of Santos, Cooray & Knox (2004), are found for other models. The reionization model provides information on \bar{x}_e and ionizing source bias. In Fig. 1, we separate the contribution to the 21 cm anisotropy power spectrum to those related to the neutral density/ionizing fraction fields (P_{aa}) and peculiar velocities (P_{bb}). In addition to these two, the cross spectra between these quantities (P_{ab}) also contribute to the total 21 cm anisotropy angular power spectrum and this leads to a roughly a factor of 2 increase in power at large angular scales when compared to density fluctuations alone.

In the bottom panel of Fig. 1, we show how this fraction varies as a function of the observational bandwidth. In addition to the ratio of total to density contributions, we also show the fractional contribution related to peculiar velocity fluctuations alone. For all bandwidths, this contribution is at the level around 0.3; one cannot simply ignore the presence of peculiar velocities based on assumptions related to a large bandwidth for observations (c.f., Zaldarriaga, Furlanetto & Hernquist 2004). Note that the importance of peculiar velocities has already been discussed in Bharadwaj & Ali (2004) in the context of 21 cm fluctuations prior to reionization in the form of an absorption signal related to background CMB.

2.1 Power spectrum covariance

In prior works related to the 21 cm anisotropies, the fluctuations were assumed to be Gaussian so that the power spectrum captures all statistical information and its variance is simply given by Gaussian statistics (e.g., Zaldarriaga, Furlanetto & Hernquist 2004; Santos, Cooray & Knox 2004). The second order corrections to the 21 cm brightness temperature, in an era of partial reionization, however, leads to a non-Gaussian contribution to the 21 cm brightness temperature anisotropies. These non-Gaussianities, then, add an extra covariance component to the power spectrum measurement and a reliable estimate of the signal-to-noise ratio of the power spectrum measurement should account for these, and other potentially interesting, non-Gaussian effects.

Writing the measured power spectrum as

$$\hat{C}_l = \frac{1}{2l+1} \sum_{m=-l}^l \langle a_{lm} a_{lm}^* \rangle, \quad (16)$$

we note that the full covariance of this measured power spectrum is

$$\begin{aligned} \text{Cov}_{l_1 l_2} &= \\ &= \frac{1}{2l_1+1} \frac{1}{2l_2+1} \sum_{m_1 m_2} \langle a_{l_1 m_1} a_{l_1 m_1}^* a_{l_2 m_2} a_{l_2 m_2}^* \rangle - \hat{C}_{l_1} \hat{C}_{l_2}, \end{aligned} \quad (17)$$

and separate this to part which is Gaussian and a part which is non-Gaussian such that

$$\begin{aligned} \text{Cov}_{l_1 l_2} &= \text{Cov}_{l_1 l_2}^{\text{Gau}} + \text{Cov}_{l_1 l_2}^{\text{NG}} \\ \text{Cov}_{l_1 l_2}^{\text{Gau}} &= \frac{2}{2l_1+1} C_{l_1}^2 \delta_{l_1 l_2} \\ \text{Cov}_{l_1 l_2}^{\text{NG}} &= \frac{1}{2l_1+1} \frac{1}{2l_2+1} \sum_{m_1 m_2} \langle a_{l_1 m_1} a_{l_1 m_1}^* a_{l_2 m_2} a_{l_2 m_2}^* \rangle_c, \end{aligned} \quad (18)$$

where $\langle \dots \rangle_c$ denotes the connected part of the four-point correlator. To calculate this non-Gaussian part, we now make use of the second order correction and, here, only focus on the part involving the convolution between neutral Hydrogen density and ionization fraction fluctuations. In terms of multipole moments, this second order term can be written as

$$\begin{aligned} a_{lm}^2 &= -(4\pi)^2 \int \frac{d^3 \mathbf{k}_1}{(2\pi)^3} \int \frac{d^3 \mathbf{k}_2}{(2\pi)^3} \sum_{l_1 m_1} \sum_{l_2 m_2} (-i)^{l_1+l_2} \\ &\times \int dr c \bar{x}_e j_{l_1}(k_1 r) j_{l_2}(k_2 r) \delta_x(\mathbf{k}_1) \delta_g(\mathbf{k}_2) \\ &\times Y_{l_1}^{m_1*}(\hat{\mathbf{k}}_1) Y_{l_2}^{m_2*}(\hat{\mathbf{k}}_2) \int d\hat{\mathbf{n}} Y_l^{m*}(\hat{\mathbf{n}}) Y_{l_1}^{m_1}(\hat{\mathbf{n}}) Y_{l_2}^{m_2}(\hat{\mathbf{n}}). \end{aligned} \quad (19)$$

Using this term twice, we simplify to obtain

$$\begin{aligned} \langle a_{l_1 m_1} a_{l_1 m_1}^* a_{l_2 m_2} a_{l_2 m_2}^* \rangle_c &= \\ &= \frac{8}{\pi^3} \int k_1^2 dk_1 \int k_2^2 dk_2 \int k_3^2 dk_3 c^4 \bar{x}_e^2 \\ &\times \left[\bar{x}_e^2 P_{x_e x_e}(k_1) P_{x_e x_e}(k_2) P_{gg}(k_3) \right. \\ &\quad \left. + (1 - \bar{x}_e)^2 P_{gg}(k_1) P_{gg}(k_2) P_{x_e x_e}(k_3) \right] \end{aligned} \quad (20)$$

6 Cooray

$$\begin{aligned}
& \times \sum_{m_1 m_2 l m} I_{l_2}(k_2) I_{l_1}(k_1) K_{l_1, l}(k_1, k_3) K_{l_2, l}(k_2, k_3) \\
& \times \int d\hat{\mathbf{n}} Y_{l_1}^{m_1}(\hat{\mathbf{n}}) Y_{l_2}^{m_2}(\hat{\mathbf{n}}) Y_l^m(\hat{\mathbf{n}}) \\
& \times \int d\hat{\mathbf{m}} Y_{l_2}^{m_2}(\hat{\mathbf{m}}) Y_{l_1}^{m_1}(\hat{\mathbf{m}}) Y_l^m(\hat{\mathbf{m}}),
\end{aligned}$$

where

$$K_{l_1, l_2}(k_1, k_2) = \int dr W_\nu(r) j_{l_1}(k_1 r) j_{l_2}(k_2 r). \quad (21)$$

Including permutations, the non-Gaussian part of the power spectrum covariance is then

$$\begin{aligned}
\text{Cov}_{l_1 l_2}^{\text{NG}} = & \quad (22) \\
& \frac{8}{\pi^4} \sum_l (2l+1) \begin{pmatrix} l_1 & l_2 & l \\ 0 & 0 & 0 \end{pmatrix}^2 \int k_1^2 dk_1 \int k_2^2 dk_2 \\
& \times \int k_3^2 dk_3 c^4 \bar{x}_e^2 \left[\bar{x}_e^2 P_{x_e x_e}(k_1) P_{x_e x_e}(k_2) P_{gg}(k_3) \right. \\
& \quad \left. + (1 - \bar{x}_e)^2 P_{gg}(k_1) P_{gg}(k_2) P_{x_e x_e}(k_3) \right] \\
& \times I_{l_2}(k_2) I_{l_1}(k_1) K_{l_1, l}(k_1, k_3) K_{l_2, l}(k_2, k_3),
\end{aligned}$$

and an additional permutation with the replacement of $l_1 \rightarrow l_2$. Here, in simplifying, we have made use of the orthonormality relation between Wigner-3j symbols. Note that we have ignored the cross power spectra between density and ionization fraction here since these are likely to be subdominant relative to the density and ionization fraction power spectra alone. Furthermore, we have ignored the non-Gaussian signals associated with the coupling between density fluctuations and peculiar velocities. These are subdominant due to mismatch in projection between density and velocity fluctuations, captured by projection integrals of I_l with a j_l , and J_l with a j_l'' .

In Fig. 1, we show the variance related to Gaussian cosmic variance term and the non-Gaussian contribution separately in the form of an error on the measured power spectrum and unbinned in multipole space. These errors are equivalent to that of $\sqrt{\text{Cov}_{ll}}$ but weighted by a factor of $l(l+1)/2\pi$. As shown, the non-Gaussian correction to the unbinned power spectrum measurement error is two orders of magnitude below when compared to that due to Gaussian errors.

In Fig. 2, we show the correlation coefficient related to the non-Gaussian covariance where we plot $\text{Corr} = \text{Cov}_{l_1 l_2}^{\text{NG}} / \sqrt{\text{Cov}_{l_1 l_2}^{\text{NG}} \text{Cov}_{l_2 l_1}^{\text{NG}}}$ as a function of l_2 for several values of l_1 . While these correlations are large, note that what matters for the power spectrum measurement is the total correlations, or rather, $\text{Cov}_{l_1 l_2}^{\text{NG}} / \sqrt{\text{Cov}_{l_1 l_1} \text{Cov}_{l_2 l_2}}$. Since $\text{Cov}_{l_1 l_1} = \text{Cov}_{l_1 l_1}^{\text{Gau}} + \text{Cov}_{l_1 l_1}^{\text{NG}} \approx \text{Cov}_{l_1 l_1}^{\text{Gau}}$, these correlations are below a percent at most (when $l \sim \text{few } 10^3$) and can be ignored for all reasonable purposes involving the measurement of the 21 cm power spectrum.

2.2 Bispectrum

While corrections to the power spectrum covariance from non-Gaussianities are negligible, it is still useful to con-

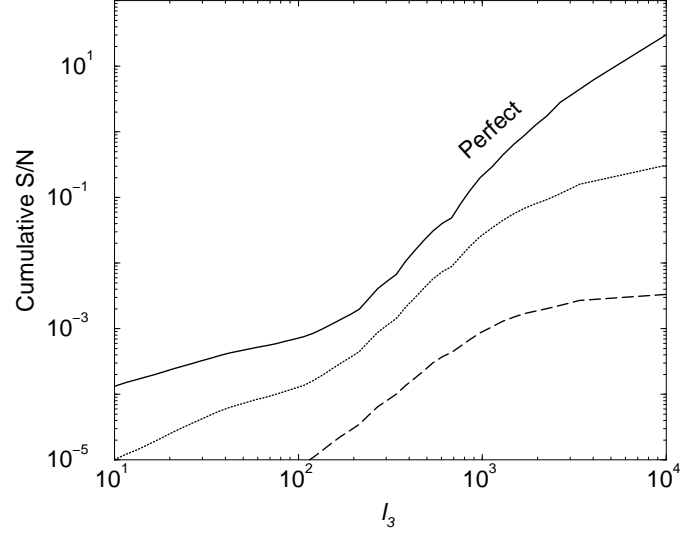


Figure 3. Cumulative signal-to-noise ratio for the measurement of the 21 cm bispectrum as a function of l_3 , for observations at $z = 10$ with a bandwidth of 1 MHz. From top-to-bottom, the three curves for an all-sky experiment with no instrumental noise, a 4000 deg.² survey with instrumental noise as show in Fig. 1, and a survey of 400 deg.² and with an increase in noise by a factor of 2 to account for unsubtracted foregrounds following Santos, Cooray & Knox (2004). While the signal-to-noise ratio is at the level of a few tens for the *perfect* experiment, for more realistic scenarios, the signal-to-noise ratio is below a unity.

sider if non-Gaussianities in the 21 cm background can be measured with upcoming interferometers. To calculate the non-Gaussian signal, here, we concentrate on the lowest order statistic and estimate the signal-to-noise ratio associated with the bispectrum, or the Fourier space analogue of the three-point correlation function. For reference, the three-point correlation function is related to multipole moments via

$$\begin{aligned}
B(\hat{\mathbf{n}}, \hat{\mathbf{m}}, \hat{\mathbf{l}}) & \equiv \langle T(\hat{\mathbf{n}}) T(\hat{\mathbf{m}}) T(\hat{\mathbf{l}}) \rangle \\
& \equiv \sum \langle a_{l_1 m_1} a_{l_2 m_2} a_{l_3 m_3} \rangle Y_{l_1}^{m_1}(\hat{\mathbf{n}}) Y_{l_2}^{m_2}(\hat{\mathbf{m}}) Y_{l_3}^{m_3}(\hat{\mathbf{l}}),
\end{aligned} \quad (23)$$

where the sum is over $(l_1, m_1), (l_2, m_2), (l_3, m_3)$. Statistical isotropy allows us to express the correlation in terms an m -independent function,

$$\langle a_{l_1 m_1} a_{l_2 m_2} a_{l_3 m_3} \rangle = \begin{pmatrix} l_1 & l_2 & l_3 \\ m_1 & m_2 & m_3 \end{pmatrix} B_{l_1 l_2 l_3}, \quad (24)$$

where the quantity $B_{l_1 l_2 l_3}$ is described as the angular averaged bispectrum (Cooray & Hu 2000) and we have made use of the orthonormality relation related to Wigner-3j symbols. As discussed in Cooray & Hu (2000), the angular bispectrum, $B_{l_1 l_2 l_3}$, contains all the information available in the three-point correlation function and frequently used quantities such as the skewness and the collapsed three-point function can be written in terms of the bispectrum, such as a filtered sum of certain bispectrum configurations (Cooray & Hu 2001a).

We consider the bispectrum formed by the 21 cm brightness fluctuations. This non-Gaussianity arises from the sec-

ond order terms in Eq. 3 (or in Fourier space, Eq. 9). Here, we again ignore the correction related to peculiar velocities, but instead focus on the second order term related to the coupling between neutral gas density fluctuations and the ionization fraction distribution. The bispectrum is simply then

$$\begin{aligned} \langle a_{l_1 m_1}^2 a_{l_2 m_2} a_{l_3 m_3} \rangle = & \\ \frac{4}{\pi^2} \int k_1^2 dk_1 \int k_2^2 dk_2 c^3 (1 - \bar{x}_e) \bar{x}_e^2 I_{l_2}(k_1) I_{l_3}(k_2) & \\ \times K_{l_2, l_3}(k_1, k_2) [P_{gg}(k_1) P_{x_e x_e}(k_2) + P_{gx_e}(k_1) P_{gx_e}(k_2)] & \\ \times \int d\hat{\mathbf{n}} Y_{l_1}^{m_1}(\hat{\mathbf{n}}) Y_{l_2}^{m_2}(\hat{\mathbf{n}}) Y_{l_3}^{m_3}(\hat{\mathbf{n}}), & \end{aligned} \quad (25)$$

where, again, we have made use of the $a_{l m}^2$ term from Eq. 19.

The bispectrum is given by

$$\begin{aligned} B_{l_1 l_2 l_3} &= \sum_{m_1 m_2 m_3} \begin{pmatrix} l_1 & l_2 & l_3 \\ m_1 & m_2 & m_3 \end{pmatrix} [\langle a_{l_1 m_1}^2 a_{l_2 m_2} a_{l_3 m_3} \rangle + \text{Perm.}] \\ &= \sqrt{\frac{(2l_1 + 1)(2l_2 + 1)(2l_3 + 1)}{4\pi}} \begin{pmatrix} l_1 & l_2 & l_3 \\ 0 & 0 & 0 \end{pmatrix} \\ &\quad \times [b_{l_2, l_3} + \text{Perm.}]. \end{aligned}$$

Here,

$$\begin{aligned} b_{l_2, l_3} &= \frac{4}{\pi^2} \int k_1^2 dk_1 \int k_2^2 dk_2 c^3 (1 - \bar{x}_e) \bar{x}_e^2 \\ &\quad \times [P_{gg}(k_1) P_{x_e x_e}(k_2) + P_{gx_e}(k_1) P_{gx_e}(k_2)] \\ &\quad \times I_{l_2}(k_1) I_{l_3}(k_2) K_{l_2, l_3}(k_1, k_2). \end{aligned} \quad (27)$$

The permutations here account for the 3 additional terms with the replacement of $l_2 \rightarrow l_3$ and l_1 .

The signal-to-noise ratio for the bispectrum is calculated as

$$\left(\frac{S}{N}\right)^2 = f_{\text{sky}} \sum_{l_3 \geq l_2 \geq l_1} \frac{(B_{l_1 l_2 l_3})^2}{C_{l_1}^{\text{tot}} C_{l_2}^{\text{tot}} C_{l_3}^{\text{tot}}}, \quad (28)$$

Here, C_l^{tot} represents all contributions to the power spectrum of the i th field,

$$C_l^{\text{tot}} = C_l + C_l^{\text{noise}} + C_l^{\text{foreg}}, \quad (29)$$

where C_l^{noise} is the instrumental noise contribution related to a 21 cm observations, and C_l^{foreg} is the confusing foreground contribution. The expression assumes all-sky observations of the 21 cm background, but in the case of partial sky observations, the square of the signal-to-noise ratio is reduced by the fraction of sky covered by the data, f_{sky} . We make use of the noise spectrum shown in Fig. 1 and include foregrounds in terms of the residual noise left over after multi-frequency cleaning following Santos, Cooray & Knox (2004). This procedure generally results in a factor of ~ 2 increase in instrumental noise in the mutlipole range of general interest.

In Fig. 3, we summarize our results related to the signal-to-noise ratio calculation. While the signal-to-noise ratio is at the level of a few tens for a no instrumental noise experiment that map out essentially the all sky, for partial sky-coverages and for added instrumental and foreground noise, the signal-to-noise ratio decreases below a unity suggesting

that a reliable detection of the 21 cm anisotropy bispectrum may not be possible with first-generation low-frequency radio interferometers.

3 DISCUSSION & SUMMARY

The brightness temperature fluctuations in the 21 cm background related to neutral Hydrogen content provide a useful probe of physics related to the era of reionization during the transition from a completely neutral intergalactic medium to a partially ionized one. Here, we have presented a complete description of brightness temperature anisotropies related to 21 cm background in terms of fluctuations in the spatial distribution of density, peculiar velocity and ionization-fraction. Our calculations are more appropriate to the large physical, and thus large angular, scales since we have not attempted to model the small-scale non-linear behavior of the reionization process as well as effects associated with finite size of ionizing patches, among others.

Our formalism allows us to calculate the angular power spectrum, the bispectrum, the Fourier analog of the three-point correlation function, and the trispectrum, the Fourier analog of the four-point correlation function, of 21 cm fluctuations. In the case of the power spectrum, we have shown that peculiar velocities cannot easily be ignored since variations in the large scale velocity field and its cross-correlation with the density distribution lead to an additional contribution to the angular power spectrum of 21 cm anisotropies. For simple models related to the correlation between density and velocity fluctuations, the correction is at the level of a factor of 2. As shown in Fig. 1, at large angular scales, this correction is independent of the bandwidth of 21 cm observations while with increasing bandwidth, the correction reduces at arcminute angular scales corresponding to multipoles of a 10^3 and higher.

We also extend previous discussions related to the power spectrum measurement by including an estimate of the non-Gaussian covariance resulting from parallelogram configurations of the trispectrum. In the case of the variance, in terms of an unbinned error on the power spectrum, the non-Gaussian correction is at least two orders of magnitude at degree angular scales with an increase to slightly less than an order of magnitude at multipoles of 10^4 (Fig. 1). In the case of the covariance, in terms of correlations between power spectrum measurements at different multipoles, the correlations are at most at the level of a few percent, when $l \sim 10^4$, suggesting that for most practical purposes non-Gaussianities can be safely ignored. While the effect of non-Gaussianities on the power spectrum measurement is insignificant, in terms of a direct measurement of the non-Gaussian signal, we have explore the possibility related to a measurement of the bispectrum. As shown in Fig. 3, the signal-to-noise ratio for the full bispectrum measurement is at most at the level of a few tens. For more practical observations with the first generation experiments, this ratio drops below unity both due to added instrumental noise and the small sky-coverage. It is unlikely that the non-Gaussian signal will be directly measurable with 21 cm data alone.

It could be possible to pull out additional information, especially related to the non-linear mode coupling second order terms, using cross-correlations between small scale CMB anisotropies (Cooray 2004b).

Thus, for most practical purposes, the presence of non-Gaussianities can be ignored and the 21 cm fluctuations can be described with Gaussian statistics. Since 21 cm fluctuations are significantly contaminated with foregrounds, such as galactic synchrotron or low-frequency radio point sources, the lack of a significant non-Gaussianity in the signal suggests that any significant detection of non-Gaussianity can be easily ascribed to a foreground confusion. Similarly, in addition to frequency information that is now proposed to separate 21 cm fluctuations from foregrounds, if non-Gaussian structure of foregrounds is a priori known, one can potentially use this additional information to further reduce the foreground confusion. This requires a better understanding of the foreground distribution, especially involving the non-Gaussian nature of foregrounds. While in Santos, Cooray & Knox (2004), foregrounds were described only in terms of the power spectra, the formalism can be modified to include this additional information and we hope to return to this topic in a later discussion.

While our calculations show that non-Gaussianities in the 21 cm background may not be significant, we may have underestimated the non-Gaussian nature by only concentrating on the large physical, and thus large angular, scales of the signal. For example, additional non-Gaussianities are expected when the density field becomes non-linear. This, for redshifts $z \sim 10$, happens at scales below the typical resolution of upcoming instruments and can be safely ignored. Similarly, the non-linear nature of the reionization process, especially the finite patch size of reionization patches, could lead to an additional non-Gaussian signal. This again depends on model dependent quantities and are better addressed with numerical simulations rather than analytical calculations.

Acknowledgments: Author acknowledges support from the Sherman Fairchild foundation and NASA NAG5-11985.

REFERENCES

- Barkana, R. & Loeb, A. 2001, *Physics Reports*, 349, 125
 Bennett C. L., Halpern M., Hinshaw G., Jarosik N., Kogut A., Limon M., Meyer S. S., Page L., et al. 2003, *ApJS*, 583, 1
 Bharadwaj S., Ali S. S. 2004, *MNRAS*, 352, 142
 Bharadwaj S., Pandey S. K. 2004, *MNRAS* submitted (astro-ph/0410581)
 Cen R. 2003, *ApJ*, 591, L5
 Chen X., Cooray A., Yoshida N., Sugiyama N., 2003, *MNRAS*, 346, L31
 Chen X., Miralda-Escudé J. 2004, *ApJ*, 602, 1
 Ciardi, B. & Madau, P. 2003, *ApJ*, 596, 1
 Cooray A. R., Hu W., 2000, *ApJ*, 534, 533
 Cooray A. R., Hu W., 2001a, *ApJ*, 548, 7
 Cooray A. R., Hu W., 2001b, *ApJ*, 554, 56
 Cooray A. 2004a, *PRD*, 70, 023508
 Cooray A. 2004b, *PRD*, 70, 063509
 Cooray, A. & Sheth, R. 2002, *Phys. Rep.*, 372, 1
 Cooray A., Furlanetto S. 2004, *ApJ*, 606, L5
 Di Matteo, T., Perna, R., Abel, T., & Rees, M. 2002, *ApJ*, 564, 576
 Fan X., Narayanan V. K., Strauss M. A., White R. L., Becker R. H., Pentericci L., Rix H. W. 2002, *AJ*, 123, 1247
 Field, G. B. 1959, *ApJ*, 129, 525
 Gnedin, N. Y. 2004, *ApJ*, 610, 9
 Gunn J. E., Peterson B. A., *ApJ*, 142, 1633
 Haiman, Z., & Holder, G. P. 2003, *ApJ*, 595, 1
 Hu W., Holder G. P., 2003, *PRD*, 68, 023001
 Kaiser N., 1992, *ApJ*, 388, 272
 Kaplinghat M., Chu M., Haiman Z., Holder G. P., Knox L., Skordis C., 2003, *ApJ*, 583, 24
 Kogut A., Spergel D. N., Barnes C., Bennett C. L., Halpern M., Hinshaw G., Jarosik N., Limon M., Meyer S. S., Page L. et al. 2003, *ApJS*, 148, 1 61
 Loeb A., Zaldarriaga M., 2004, *PRL*, 92, 211301
 Madau, P., Meiksin, A., & Rees, M. J. 1997, *ApJ*, 475, 429
 Mo, H. J., Jing, Y. P., White, S. D. M. 1997, *MNRAS*, 284, 189
 Morales, M. F. & Hewitt, J. 2004, *ApJ*, 615, 7
 Oh, S. P., & Mack, K. J. 2003, *MNRAS*, 346, 871
 Oh, S. P. 1999, *ApJ*, 527, 16
 Pen U., Wu X., Peterson J. B., 2004, astro-ph/0404083
 Santos, M. G., Cooray, A., Haiman, Z., Knox, L., & Ma, C.-P. 2003, *ApJ*, 598, 756
 Santos M. G., Cooray, A., Knox L., 2004, *ApJ* submitted, astro-ph/0408515
 Scoccimarro R., Zaldarriaga M., Hui L., 1999, *ApJ*, 527, 1
 Scott, D., & Rees, M. J. 1990, *MNRAS*, 247, 510
 Shaver P. A., Windhorst R. A., Madau P., de Bruyn A. G. 1999, *A&A*, 345, 380
 Spergel, D. N., et al. 2003, *ApJS*, 148, 175
 Venkatesan A., Giroux M. L., Shull J. M. 2001, *ApJ*, 563, 1
 Zaldarriaga, M., 1997, *PRD*, 55, 1822
 Zaldarriaga, M., Furlanetto, S. R., Hernquist, L. 2004, *ApJ*, 608, 622
 Wyithe J. S. B., Loeb A. 2003, *ApJ*, 588, L69